Supplementary Information for

Biomolecule-derived three-dimensional N, P co-doped carbon nanosheets for efficient oxidative dehydrogenation of propane

Ziyi Chen, [a] Xiaomin Zhang, [a] QiWei Duan, [a] Guangming Wang, [a] Shuchun Li, [a] KaiHua Yu, [a] Changsheng Cao*[a] and Zailai Xie*[a]

[a]Key Laboratory of Advanced Carbon-Based Functional Materials (Fujian Province University), Fuzhou University, Fuzhou 350108, China

*Corresponding Author E-mail: cscao@fzu.edu.cn; zlxie@fzu.edu.cn

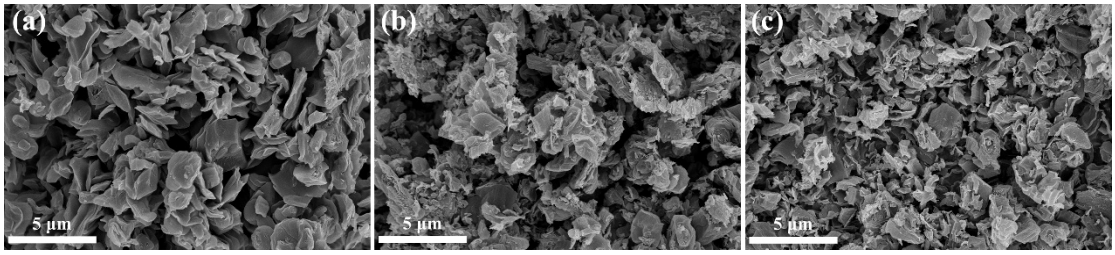

Fig. S1. SEM images of (a) NPC-NSs-T, (b) NPC-NSs-P and (c) NC-NSs.

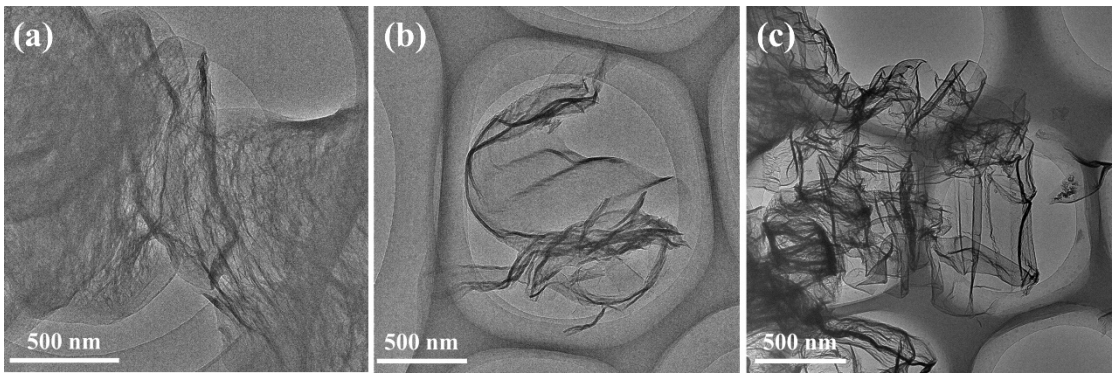

Fig. S2. TEM images of (a) NPC-NSs-T, (b) NPC-NSs-P and (c) NC-NSs.

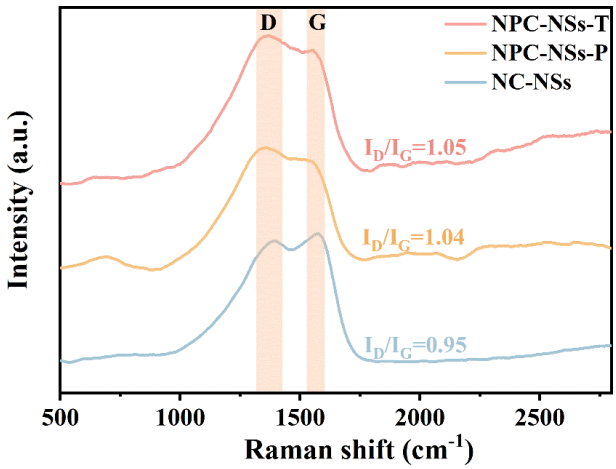

Fig. S3. Raman spectra of NPC-NSs-T, NPC-NSs-P and NC-NSs.

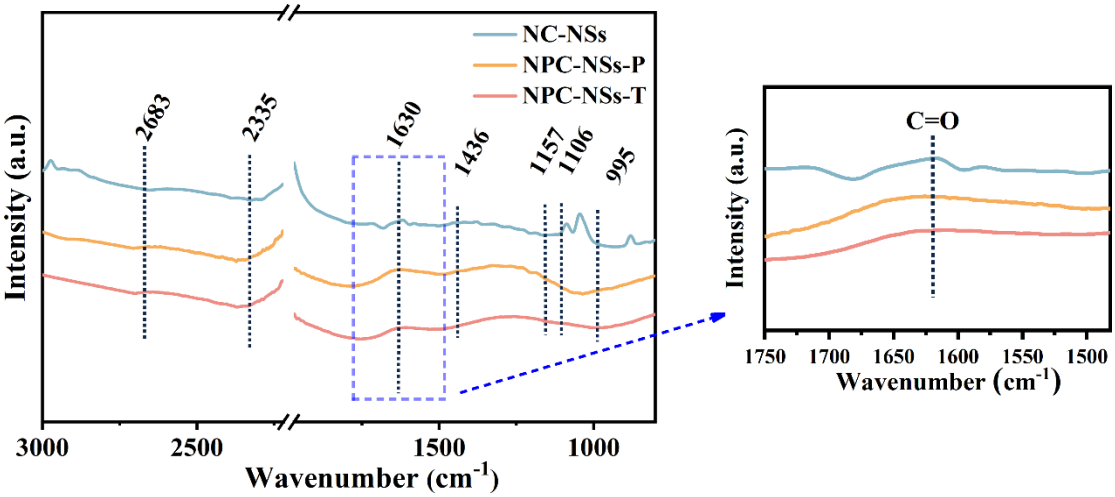

Fig. S4. FT-IR spectra of NPC-NSs-T, NPC-NSs-P and NC-NSs.

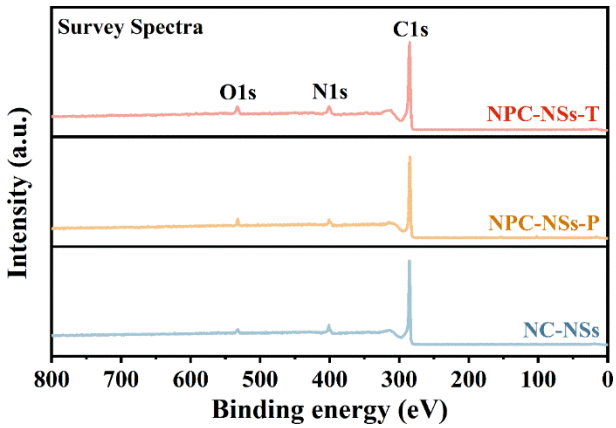

Fig. S5. XPS survey spectra of NPC-NSs-T, NPC-NSs-P and NC-NSs.

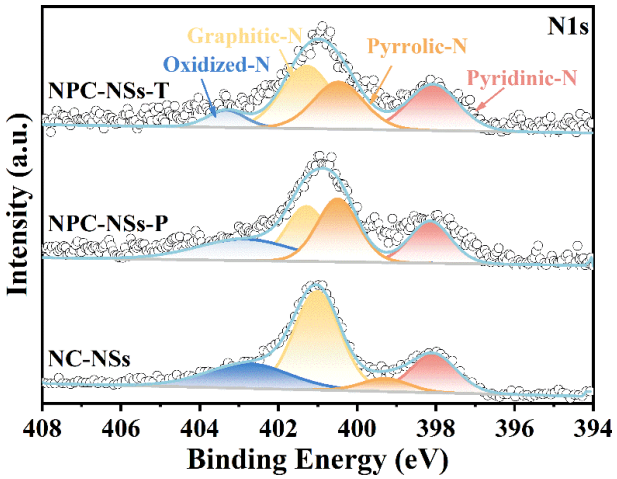

Fig. S6. N 1s XPS spectra of NPC-NSs-T, NPC-NSs-P and NC-NSs.

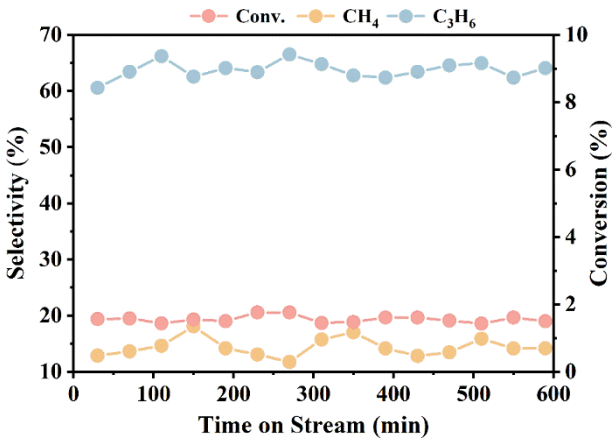

Fig. S7. Catalytic performance of pure quartz at 500 °C.

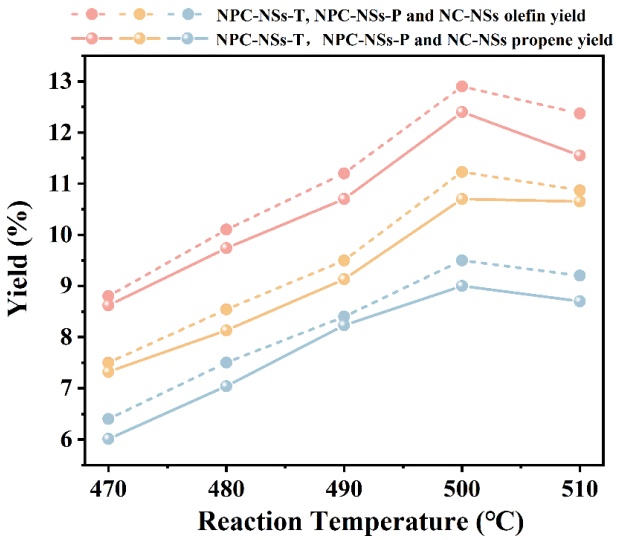

Fig. S8. Propene and olefin yield of NPC-NSs-T, NPC-NSs-P and NC-NSs at different reaction temperatures.

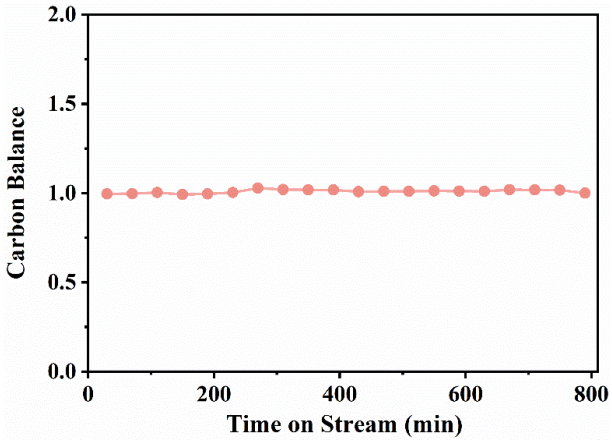

Fig. S9. Carbon balance of NPC-NSs-T during the long-term test at 500 °C.

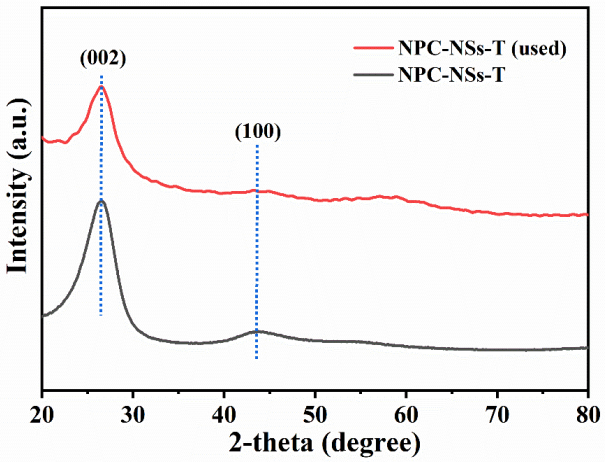

Fig. S10. PXRD patterns of NPC-NSs-T before and after reaction.

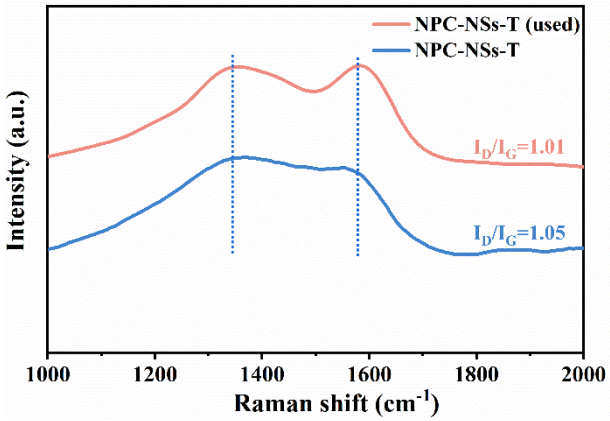

Fig. S11. Raman spectra of NPC-NSs-T before and after reaction.

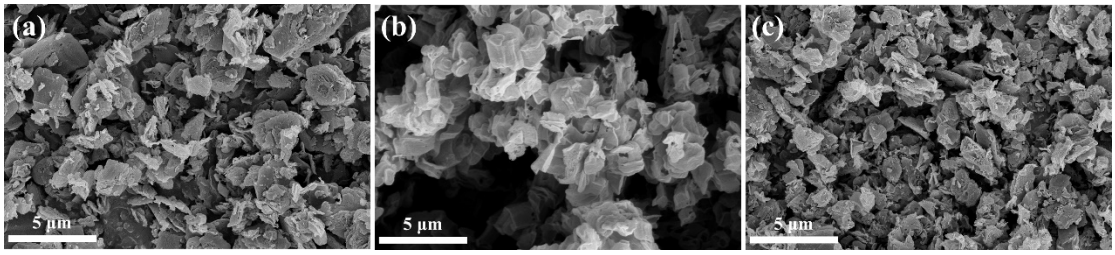

Fig. S12. SEM images of (a) NPC-NSs-T, (b) NPC-NSs-P and (c) NC-NSs after the reaction.

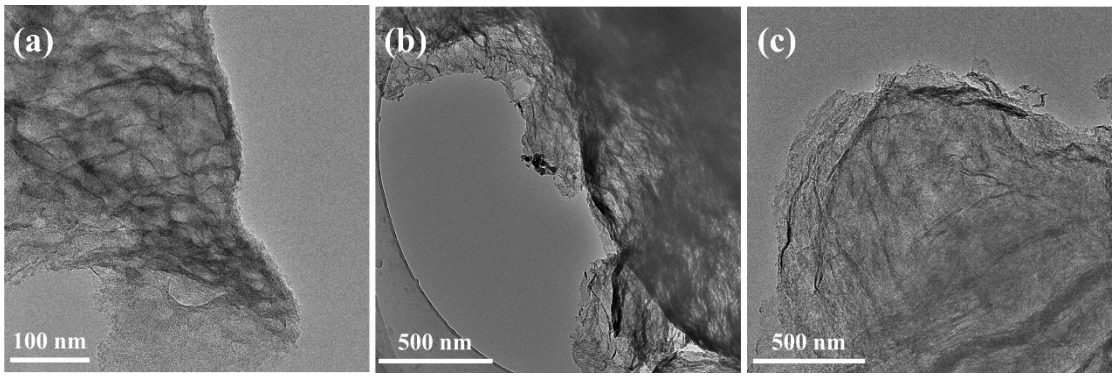

Fig. S13. TEM images of (a) NPC-NSs-T, (b) NPC-NSs-P and (c) NC-NSs after the reaction.

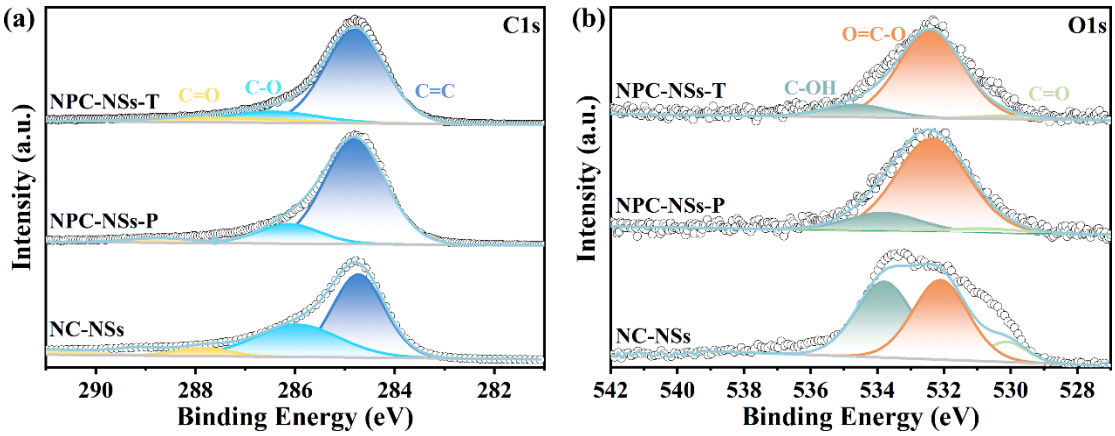

Fig. S14. (a) C 1s and (b) O 1s XPS spectra of NPC-NSs-T, NPC-NSs-P and NC-NSs after reaction.

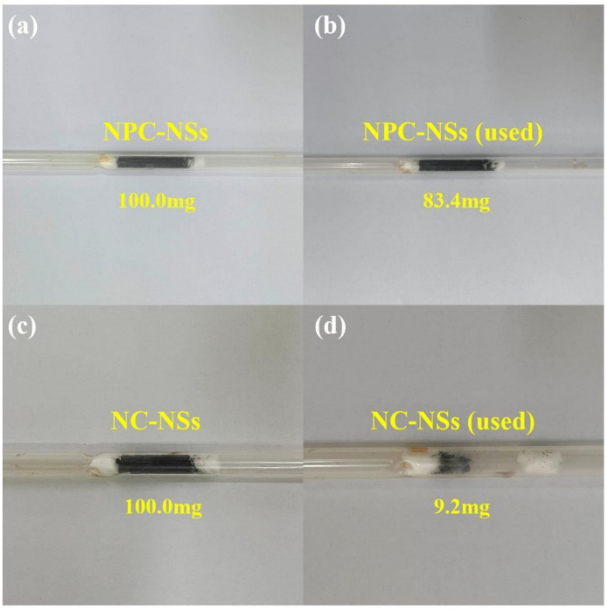

Fig. S15. Photographs of NCP-NSs and NC-NSs in the quartz tube before (a, c) and after (b, d) reaction.

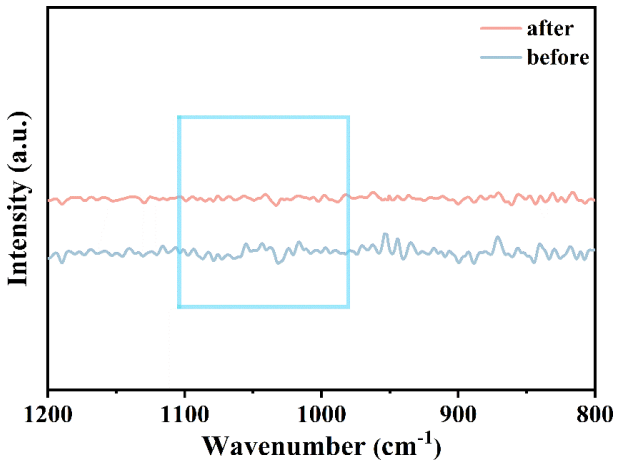

Fig. S16. *In-situ* DRIFTS spectra of NPC-NSs-T before and after heat treatment at 500 °C.

Notes: According to previous works, the characteristic peaks of P=O and P-O-C species are mainly located in the region of 900-1100 cm^{-1}. However, the *in-situ* DRIFTS spectra is almost the same before and after heat treatment at 500 °C. Therefore, we suppose that the P=O and P-O-C groups are stable at 500 °C.

Table S1. Micropore volume and external surface area of NC-NSs, NPC-NSs-P and NPC-NSs-T.

Samples	Micropore surface area ($cm^2 g^{-1}$)	Mesopore surface area ($cm^2 g^{-1}$)
NC-NSs	2.06	32.54
NPC-NSs-P	1.81	36.21
NPC-NSs-T	1.11	41.60

Table S2. Comparison of surface element content of NC-NSs and NPC-NSs-T before and after ODHP reactions.

Samples	Elements and species contents (at.%)			
	P*	C	O	C=O
NC-NSs		92.37	1.76	14.57
NC-NSs (uesd)		92.82	3.3	8.39
NPC-NSs-T	0.28	87.29	4.03	9.21
NPC-NSs-T (uesd)		87.88	4.76	8.71
NPC-NSs-P	0.22	88.37	2.88	4.43
NPC-NSs-P (uesd)		88.69	4.63	3.46

Note: *P contents (wt.%) were measured by ICP-OES.

Table S3. Summary of catalytic performance of some recently reported carbon-based catalysts in ODHP reactions.

Samples	Conversion (%)	Selectivity (%)	Propylene Yield (%)	Refs.
NC-NSs	18.6	51.07	9.0	
NPC-NSs-P	19.8	56.43	10.7	**This work**
NPC-NSs-T	19.94	64.16	12.4	
g-C_3N_4-12 h	14.9	74.7	11.1	[1]
PZS@OCNT	14.3	63	9.0	[2]
2% B-SFC	2.0	88.6	1.7	[3]
$B_{0.6}CN$	6.7	84.6	5.7	[4]
NG-2	10.0	55.0	5.5	[5]
CN-15-2.0	22.98	41.70	9.6	[6]

References

1. L. Cao, P. Dai, L. Zhu, L. Yan, R. Chen, D. Liu, X. Gu, L. Li, Q. Xue and X. Zhao, *Appl. Catal. B Environ.*, 2020, **262**, 118277.
2. T. Cao, X. Dai, W. Liu, Y. Fu and W. Qi, *Carbon*, 2022, **189**, 199-209.
3. T. Wang and M. Zhu, *Chinese J. Chem. Eng.*, 2023, **62**, 310-317.
4. R. Goyal, B. Sarkar, A. Bag, F. Lefebvre, S. Sameer, C. Pendema and A. Bordoloi, *J. Mater. Chem. A*, 2016, 18559-18569.
5. W. Liu, T. Cao, X. Dai, Y. Bai, X. Lu, F. Li and W. Qi, *Front. Chem.*, 2021, **9**, 759936.
6. W. Zhang, G. Zhao, T. Muschin and A. Bao, *Surf. Interface Anal.*, 2021, **53**, 100-107.